RESEARCH PAPER

PCCP
www.rsc.org/pccp

Comparison of the *cis*-bending and C–H stretching vibration on the reaction of $C_2H_2^+$ with H_2 using laser induced reactions†

Stephan Schlemmer,*[ab] Oskar Asvany[b] and Thomas Giesen[a]

[a] *I. Physikalisches Institut, Universität zu Köln, Zülpicher Str. 77, 50937 Köln, Germany. E-mail: schlemmer@ph1.uni-koeln.de*
[b] *Leiden Observatory, PO Box 9513, 2300 RA Leiden, The Netherlands*

Received 8th December 2004, Accepted 25th February 2005
First published as an Advance Article on the web 9th March 2005

Laser induced reaction (LIR) of $C_2H_2^+ + H_2$ in a 22-pole ion trap at 90 K has been employed to detect the ν_3 C–H stretching vibration and the ν_5 *cis* bending vibration of the acetylene parent ion using the wide tunability of the free electron laser FELIX. The vibrational frequency of the bending vibration, ω_5, and the corresponding Renner–Teller parameter, ε_5, are determined to be 710 cm^{-1} and 0.03, respectively. These results differ quite substantially from previous experimental work but are in line with the most recent and advanced theoretical work. The dependence of the LIR-signal of the two vibrational modes is studied systematically with respect to the laser power, storage time, and number density of the hydrogen collision partner. A reaction scheme describing all steps involved in the LIR process is set up. The corresponding rate equation system is solved numerically. From this solution the lifetimes for the vibrational excited states, $\tau_3 = (3 \pm 1)$ ms and $\tau_5 = (200 \pm 50)$ ms and the vibrational dipole moments $\mu_3 = 0.19(2)$ D and $\mu_5 = 0.21(2)$ D are determined under the assumption that the excited parent ion relaxes or reacts with a net rate coefficient equal to the Langevin limit. The lifetime for the C–H stretching vibration is in agreement with a previous LIR experiment and with *ab initio* calculations. C–H stretching turns out to be about an order of magnitude more efficient than bending in promoting hydrogen abstraction. This strong mode dependence is discussed on the basis of the energetics for hydrogen abstraction and a possible inhibition of complex formation in the entrance channel of the $C_2H_2^+ \cdots H_2$ collision system.

1. Introduction

Laser induced reactions (LIR) belong to the family of "action spectroscopy" methods where the influence of the laser light on the investigated mass-selected trapped ions is monitored by detecting induced changes of the ion cloud composition in a high-efficiency ion counter. In the special case of LIR, changes of the rate coefficient of an endothermic ion–molecule reaction serve to detect the excitation of the parent ionic species. This offers not only the possibility of doing very high sensitivity spectroscopy on transient ions (a number of only 1000 ions per trapping period is enough), but LIR can yield information on state-selected reaction rate coefficients and lifetimes of excited states. Examples of this method include the IR spectrum of the highly fluxional CH_5^+ molecule,[1,2] the laser induced charge transfer in the system $N_2^+ + Ar$,[3] and the IR spectroscopy of the asymmetric stretching vibration ν_3 of $C_2H_2^+$ [4] by using the abstraction reaction $C_2H_2^+ + H_2 + \hbar\omega_3 \rightarrow C_2H_3^+ + H$. In this scheme, the endothermicity of about 50 meV (= 403 cm^{-1}) is overcome by the resonant laser photon. More recently we report also on the first spectrum of the *cis*-bending vibration ν_5 of $C_2H_2^+$ using LIR.[5]

In the present work the very same reaction scheme is used to detect both the *cis*-bending vibration ν_5 and the asymmetric stretching vibration ν_3 of $C_2H_2^+$. The purpose of this study has been twofold: (i) determination of the bending vibration of $C_2H_2^+$ with a detailed examination of the rotational structure and (ii) comparison of the reactivity of the bending *versus* the stretching vibration. Ionized acetylene is an important molecule for the plasma chemistry not only in the laboratory, but also in space. Therefore a lot of experimental and theoretical work has been devoted to the spectroscopy and dynamics of $C_2H_2^+$.

Acetylene is a simple hydrocarbon molecule, linear in its neutral and ionized state. $C_2H_2^+$ is the only known example of a tetra-atomic molecule exhibiting the Renner–Teller effect in the ground state. The Renner–Teller effect, *i.e.* the splitting of the doubly degenerate electronic ground state $X^2\Pi_u$ of the linear geometry through interactions with a bending mode has only been verified experimentally for the *trans*-bending vibration ν_4,[6] but a detection for the infrared active *cis*-bending mode ν_5 with spectroscopic accuracy has been missing.

Conventional HeI photoelectron spectra (PES) from ground state neutral C_2H_2 has been used to examine the Renner–Teller structure of the ion.[7,8] Although these early experiments by Reutt *et al.* were only taken at rather poor resolution, a feature at 837 cm^{-1} above the ionization threshold has been assigned to one component of the *cis*-bending vibration ($v_5 = 1$). More recent studies used various REMPI schemes to resonantly excite the Rydberg state converging to the ionic ground state.[9–11] Both ground states of C_2H_2 and $C_2H_2^+$ are linear with slightly changing bond lengths, therefore only very weak progressions in the bending vibrations have been observed. The resonantly excited state $\tilde{A}^1A_u$ employed by Pratt *et al.*,[10] however, has *trans*-bent geometry. Therefore only the *trans*-bending vibration of $C_2H_2^+$ has been observed. Later, Pratt *et al.* refined their studies on the *trans*-bending vibrations *via* the $\tilde{A}^1A_u$ state in a two-color double resonance laser experiment.[6] Here they found three Renner–Teller components for the *trans*-bending vibration ($v_4 = 1$) at $^2\Sigma^- = 485$ cm^{-1}, $^2\Sigma^+ = 903$ cm^{-1} and $^2\Delta = 668$ cm^{-1}, with spin–orbit splitting and rotational constants similar to the ground state, *i.e.* $A \sim -30$ cm^{-1} and $B = 1.1$ cm^{-1}. Using the theoretical treatment of

† Presented at the Bunsen Discussion on Chemical Processes of Ions, Marburg, 15–17 September 2004.

DOI: 10.1039/b418495p

Petelin and Kiselev[12] they obtained a frequency of the *trans*-bending vibration of $\nu_4 = 694$ cm^{-1} and a Renner–Teller parameter $\varepsilon_4 = 0.30$. It is interesting to note that they also detected a weak feature at 748 cm^{-1} which they tentatively assigned to the $^2\Sigma^-$ component of the *cis*-bending vibration ($v_5 = 1$). This value deviates substantially from the former result by Reutt *et al.*[7] Both results could only be consistent if both experiments were detecting different Renner–Teller components ($^2\Sigma^{\pm}$) which would call for a large Renner–Teller parameter ε_5. It is quite surprising that neither study reveals both components. This finding would rather suggest that the Renner–Teller splitting of the antisymmetric bending vibration is instead small and the two $^2\Sigma$ components collapse at low resolution. This idea is corroborated by the experimental LIR-spectra as well as by theoretical work.

Multiconfiguration *ab initio* methods have been employed by Lee *et al.*[13] where predictions of the Renner–Teller components have been calculated for the *cis*- and *trans*-bending vibrations. They compare reasonably well with the experimental findings for the *trans*-bending frequencies found by Pratt *et al.*[6] *Ab initio* investigations of the Renner–Teller effect beyond the Born–Oppenheimer and the harmonic approximations have been carried out over the years by Perić and Peyerimhoff.[14,15] These authors also took the spin orbit coupling which is present in the case of the $X^2\Pi_u$ ground state of the acetylene cation into account.[16] More recently a second order perturbational approach with explicit treatment of the vibronic and spin–orbit coupling has been published. These results compare very well with the former variational treatment and they also show that the approximate analytical equations by Petelin and Kiselev[12] can be applied to model experimental data.

High-resolution infrared spectra became available for the band of the asymmetric C–H stretching vibration in the three isotopic acetylene ions $C_2H_2^+(\nu_3)$, $^{13}C_2H_2^+(\nu_3)$, and $C_2HD^+(\nu_1)$ by using a difference frequency laser spectrometer probing an AC glow discharge.[17,18] From the study of Jagod *et al.*[18] high accuracy values of the vibrational frequencies, the rotational and spin–orbit constants of the vibronic ground and excited state have been derived. However, until recently no spectra were available for the other IR active ν_5 *cis* bending vibration. The LIR spectroscopy experiment described here in more detail has been set up to obtain ro-vibrational spectra in the range of the bending vibrations between 600 and 950 cm^{-1}, and a first spectrum has already been published.[5]

In LIR experiments the collision with the neutral reaction partner is an integral part of the detection scheme. The reactivity is strongly dependent on the level of excitation. Due to the selected excitation, the LIR signal carries information about the mode selectivity of the reaction. Since nuclear rearrangement is associated with most chemical reactions it is very interesting to investigate the influence of vibrational motions on the reactivity. In former studies a comparison of the bending and C–C stretching vibration as well as collision energy effects on the reaction of $C_2H_2^+$ with D_2 has been carried out by Chiu *et al.*[19] In these experiments, $C_2H_2^+$ ions have been prepared by multiphoton ionization with excitation in either the ν_2 C–C stretch vibration or in a combination of ground state and two quanta of bending vibration. The so prepared ions interacted with the neutral reactant in a guided ion beam apparatus at selected collision energies. Formation of $C_2H_3^+$ in its isotopic forms is found to be enhanced by collision energy and C–C stretch vibration, but not by bending vibration. In addition hydrogen exchange which is an additional reaction channel is inhibited by both collision energy and vibrational energy. These results are in agreement with earlier state-selected experiments of Honma *et al.*[20] These findings could be explained with an inhibition of $C_2H_4^+$ complex formation in case of vibrational excitation. In a previous LIR experiment on the ν_3 C–H stretching vibration,[4] the branching ratio between reaction of the laser excited species and quenching has been determined to be roughly 1 : 5. This dominance of quenching *versus* reaction is in line with the idea of Chiu *et al.*[19] that the reaction is hindered due to a process happening in the entrance channel.

In the present work a comparison between the *cis*-bending vibration and the C–H stretching vibration becomes possible due to the wide tunability of the free electron laser FELIX, which allows the excitation of cold parent $C_2H_2^+$ ions in all IR active modes. The paper is organized as follows: In the experimental section the basics of the trapping experiment and the capabilities of FELIX are described. The obtained spectra and the details for the modeling of the ro-vibrational spectrum of the *cis*-bending vibration including Renner–Teller splitting are given in Section 3. In Section 4 a kinetic model describing the reaction system is laid out. Numerical simulations based on this simple model are then used in the following result Section 5 for the interpretation of the data and in particular for comparing the bending *versus* the C–H stretching vibration. Finally the LIR process is discussed (Section 6) in terms of an interpretation of the spectral intensities and the dynamical implications derived from the kinetics modelling. Conclusions for future experiments round off this paper.

2. Experimental

2.1. Basics of LIR

The experimental setup used for LIR is explained in Fig. 1. Details of the trapping technique are described thoroughly in ref. 21. The method is based on storing mass-selected ions in an environment of a cold reactant gas. For this, the ions are generated and collected in a storage ion source, from where a packet of slow ions is sent through a quadrupole mass filter for mass selection into the 22-pole ion trap. In this trap, the ions are cooled down to the desired temperature by a short He gas pulse and stored for several seconds. The trap is constantly filled with a suitable reactant gas. For LIR-spectroscopy to work, the reaction between the ions and the gas should have a barrier on the reaction pathway or be endothermic. The barrier or the endothermicity can be overcome when the ions are resonantly excited by tunable laser light. Thus, by counting

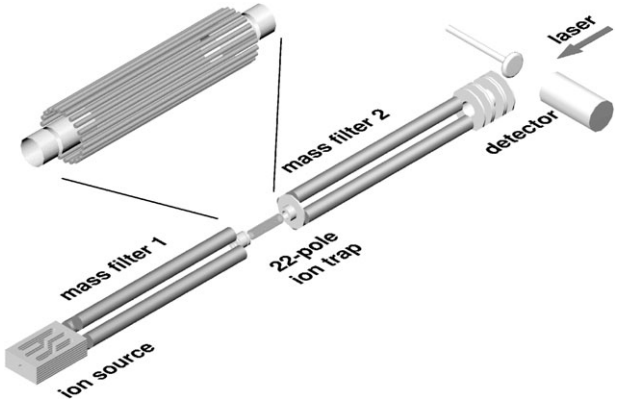

Fig. 1 Setup of the trapping apparatus as used for laser induced reactions (LIR). The ions are generated and collected in the storage ion source, mass selected in the quadrupole mass filter 1 and then stored in the 22-pole ion trap. As shown in the enlarged inset, this trap consists of 22 small rods which confine the ions in the radial direction when suitable rf voltages (~17 MHz, 50 V) are applied. Control of the injection and extraction of the ion cloud is achieved by the innermost electrodes. On entrance, the ions are cooled down to the ambient cryogenic temperature by a short intense helium pulse. During the storage period of several seconds, the ions are subject to reactant gas molecules and tunable laser light (coming from the right through the axially transparent setup). The result of this interaction is detected by extracting the stored ion cloud into mass filter 2 and counting the number of product ions in the detector. By repeating this process while scanning the IR laser, an IR action spectrum of the stored parent ions is recorded.

the mass-selected ionic reaction products as a function of the laser wavelength, a LIR spectrum is recorded. In the following subsections, more details are given for the basic reaction schemes, the ion preparation, the 22-pole trap, and the laser source FELIX.

2.2. Reactions

In the present contribution, the dynamics of the LIR-process for the IR-active *cis*-bending vibration ν_5 and asymmetric stretch ν_3 of $C_2H_2^+$ are reported. Some details of the corresponding LIR-spectra have been already summarized by Asvany *et al.*[5] and Schlemmer *et al.*[4] For LIR of the acetylene cation, $C_2H_2^+$, the H-atom abstraction reaction

$$C_2H_2^+ + H_2 \xrightarrow{k} C_2H_3^+ + H \qquad (1)$$

has been utilized. This reaction is endothermic by about 50 meV ($\sim$403 cm^{-1}), thus its rate coefficient k is very small at low temperatures. This fact renders LIR-spectroscopy feasible by first exciting the ion

$$C_2H_2^+(v_i = 0,J'') + \hbar\omega_i \rightarrow C_2H_2^+(v_i = 1,J') \qquad (2)$$

into an IR-active vibrational motion (i = 3,5) and then counting the products of the reaction

$$C_2H_2^+(v_i = 1, J') + H_2 \xrightarrow{k^*} C_2H_3^+ + H. \qquad (3)$$

Usually, the reaction is substantially enhanced by the laser excitation, *i.e.* $k^* \gg k$. As a small complication, at very low temperatures the loss of primary ions by radiative association

$$C_2H_2^+ + H_2 \xrightarrow{k_{rad}} C_2H_4^+ + \hbar\omega \qquad (4)$$

and also ternary association

$$C_2H_2^+ + 2H_2 \xrightarrow{k_{ter}} C_2H_4^+ + H_2 \qquad (5)$$

become important. To find an optimum for minimal loss of primary ions into these association channels or into reaction (1), trap temperatures around 90 K and hydrogen densities less than 1×10^{12} cm^{-3} have been chosen. The trapping time was typically 2–4 s. Other experimental parameters are summarized in Table 1.

2.3. Ion preparation and mass selection

The $C_2H_2^+$ ions were generated in an external rf ion storage source by electron bombardment of acetylene gas highly diluted in hydrogen with a ratio of around 1 : 100. The acetylene gas used (Indugas, purity 2.5) was purified in a dry ice/acetone trap. For ionization, electrons with low kinetic energies (<17 eV) were utilized to avoid internal excitation or fragmentation of the ions. Collecting the ions in this storage source makes it possible to operate at pressures below 10^{-5} mbar of the gas mixture. Furthermore, vibrationally excited $C_2H_2^+$ ions are removed by reactions of type (3). Non-reactive collisions with H_2 cool the acetylene cations to the source temperature of about 350 K. After extracting the ions through a pulsed electrode, they are mass selected by a quadrupole mass spectrometer and injected into the 22-pole ion trap where they are finally cooled to the desired low temperature by a short intense He pulse ($\sim$10 ms).

Table 1 Typical conditions for LIR-spectra shown in Fig. 2 and physical parameters for the LIR-process derived from numerical simulations

	Bend (ν_5)	Stretch (ν_3)
Center frequency ω/cm^{-1}	710	3136
FELIX resolution FWHM $\Delta\omega$/cm^{-1}	3	15
Number injected $C_2H_2^+$ ions	$\sim$2200	$\sim$1800
Iterations	10	8
Storage time t/s	4	2
Laser pulse power/mJ	$\sim$30	$\sim$10
Laser frequency/Hz	10	5
$10^{-11} \times$ H_2 density/cm^{-3}	1.2	1.5
Number $C_2H_3^+$ background ions	340	170
Lifetime τ/ms	(200 ± 50)	(3 ± 1)
Vibrational transition dipole moment/D	0.21 ± 0.02	0.19 ± 0.02
Integrated band intensity/cm^{-1}	9209	4242
k_3^*/k_5^*	7	

2.4. 22-Pole ion trap

The central part of the experiment, the 22-pole ion trap, is shown schematically in the enlarged inset in Fig. 1. It consists of 22 stainless steel rods, each 1 mm in diameter and 36 mm long, circumscribing a circle of 10 mm diameter. The rods are alternately connected to a supply electrode each of which connected to the two ends of an inductive coil (11 rods to each end), forming a LC-circuit with a resonance frequency of 17 MHz. This circuit is excited by an external rf generator. The hereby generated rf field in the trap confines the ions in the radial direction, while confinement in axial direction and the control of ion filling and extraction is achieved by the shown inner cylindrical electrodes. The shown outer electrodes are used for focusing the ion beam. The structure is surrounded by a copper box (not shown) which can be cooled to 10 K *via* a closed cycle refrigerator. The reactant gases and He pulses are admitted to the inside of the trap region by pre-cooled tubes. The number density of the target gas has been determined from the pressure increase in the trap chamber. The relation between number density at the trap temperature and pressure in the trap chamber has been carefully calibrated.

2.5. Laser source

The experiments were performed with the Free Electron Laser for Infrared eXperiments FELIX.[22] FELIX is capable of delivering pulsed infrared radiation tunable in the range from 40 cm^{-1} to 2000 cm^{-1}, and using third harmonic generation even above 3000 cm^{-1}. Tuning of the laser wavelength (in a limited range) can be made by the user by moving the undulator gap. The wavelength setting can be controlled by a spectrum analyzer contained in the FELIX beamline. This spectrum analyzer has been used to calibrate the wavelength scale of the experiment. Reproducibility, precision and accuracy are of similar size ($\sim$4 cm^{-1}). The maximum repetition rate of the macropulses, 10 Hz, has been chosen, and the pulses have a typical length of 7 μs, with a 1 GHz microstructure (in all presented cases) originating from electron bunching in the linear accelerator. The macropulses have an energy content up to 30 mJ, giving a cw power in the range of 300 mW at the user side. The resolution of FELIX was bandwidth–limited and on the order of 0.5% FWHM, *i.e.* the typical bandwidth in our experiment was $\Delta\omega = 15$ cm^{-1} (FWHM) in the C–H stretching region (3100 cm^{-1}) and about $\Delta\omega = 3$ cm^{-1} (FWHM) around 700 cm^{-1}.

At the user station, the IR radiation has been coupled into the 22-pole trapping machine *via* two mirrors and a ZnSe window. The laser pulses of FELIX and the ion pulses of the 22-pole trapping machine have not been synchronized. This is not necessary due to the long ion trapping time of several seconds and the high macropulse repetition frequency.

3. Spectroscopy

The LIR spectrum of the *cis*-bending (600–950 cm^{-1}) and the C–H stretching vibration (2800–3200 cm^{-1}) of $C_2H_2^+$ is shown in Fig. 2. The C–H stretching region around 3150 cm^{-1} has

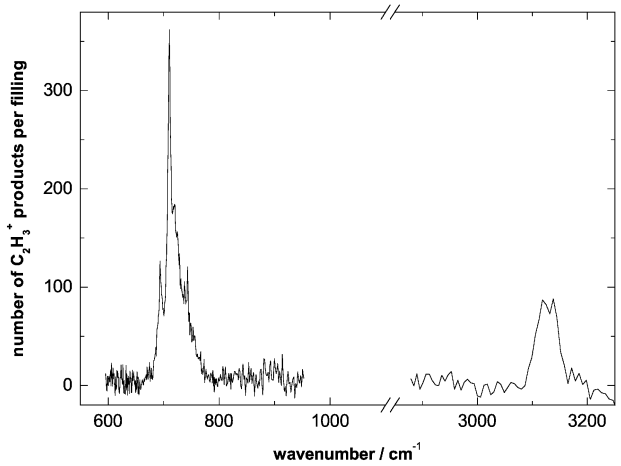

Fig. 2 Raw LIR-spectra of the IR-active bending and stretching modes of $C_2H_2^+$ as obtained by counting the number of $C_2H_3^+$ product ions of reaction (3) as a function of the FELIX laser frequency. Per storage cycle, around 2000 $C_2H_2^+$ parent ions have been trapped for several seconds in the cold 90 K hydrogen gas environment, in which they were subject to the FELIX laser pulses. For better statistics, up to ten iterations have been recorded. The background counts due to hot $C_2H_2^+$ parent ions coming from the source were subtracted in this figure. The experimental conditions used for the detection of these two vibrational modes are summarized in Table 1.

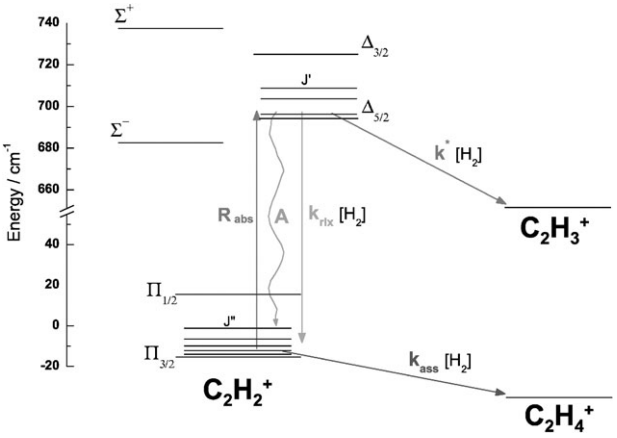

Fig. 4 Energy level diagram displaying the most important kinetic steps in the LIR-process of the *cis*-bending motion of $C_2H_2^+$. The kinetic processes and their corresponding rates are shown for the $\Delta_{5/2}$–$\Pi_{3/2}$ transition at 710 cm^{-1}. These are absorption of a laser photon (rate R_{abs}), relaxation back into the ground state either by collision with a H_2 molecule ($k_{rlx}[H_2]$) or by fluorescence (rate A). Reaction of ground state $C_2H_2^+$ with H_2 to yield $C_2H_3^+$ is very slow (thus not shown) as it is endothermic by about 400 cm^{-1}, but an excited molecule can react ($k^*[H_2]$). At the low temperatures of the experiment, association loss reactions ($k_{ass}[H_2]$) have to be taken into account.

been observed in high resolution before by Jagod *et al.*[18] and by a previous LIR study.[4] Despite the poor resolution of the present experiment it is gratifying to see that LIR works with the use of quite different laser excitation schemes. More importantly the lower frequency spectrum shows the detection of the ν_5 bending vibration of $C_2H_2^+$. This spectrum exhibits a main peak at 710 cm^{-1} with a full extension of signal from 650–780 cm^{-1}. This region is shown in more detail in Fig. 3. Here a distinct substructure becomes apparent. No intensity is observed outside this range. In particular no LIR signal is detected at the proposed value of 837 cm^{-1}.[7,23] Instead the spectrum lies in the range of the previously observed weak band detected by Pratt *et al.*[6] and assigned to the Σ^- component of the *cis* bending vibration. Without any analysis the comparably narrow LIR spectrum shows that all vibronic components of the vibrational transition fall in this frequency range, indicating that the size of the Renner–Teller parameter, ε_3, for the *cis*-bending vibration is rather small. Assuming that some vibronic components would lie even outside the wide spectral range covered in this experiment, leads to a rather large Renner–Teller parameter, $\varepsilon_3 \geq 0.3$. This finding would be in great contrast to the most advanced calculations available.[15] Therefore for the current analysis it is assumed that the full spectrum is covered by the spectrum shown in Fig. 2.

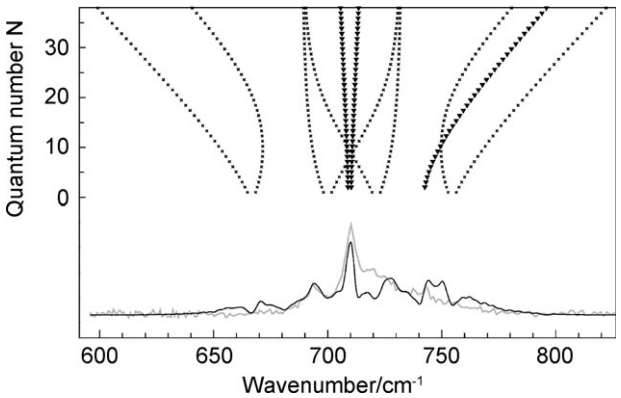

Fig. 3 Fortrat diagram of the ν_5 Q-branches of $C_2H_2^+$ (upper panel). Triangles indicate Δ–Π transitions, crosses the Σ–Π Q-branches. The measured (grey curve) and the simulated spectrum (black curve) are shown in the lower panel. Molecular parameters of the simulated spectrum are given in Table 2.

Due to the limited resolution of the spectrum shown in Fig. 3 the rotational structure is buried in the envelopes connecting the peak structure described above. In order to determine reliable values for the frequency of the ν_5 vibration and the associated Renner–Teller parameter the vibronic spectra have been simulated. The coarse structure of the spectrum is governed by the energy level diagram for the vibrational ground and first excited state of the $X^2\Pi$ electronic state of $C_2H_2^+$. The term energies have been calculated using the perturbative description by Perić and Peyerimhoff.[24] A detailed figure of the vibronic levels can be found in ref. 5. Each vibronic state is split by the spin orbit interaction which in the present case has been assumed to vary little comparing Π, Σ and Δ. The Renner–Teller distortion leads to a further shift of the spin orbit terms of the vibronic states. However, the influence is only substantial in the Σ state while it is rather small in Δ. This is well known from several cases including the *trans* bending vibration of $C_2H_2^+$. The diagram of the vibronic states is shown in the left part of Fig. 4. For the case shown the electron spin $S = 1/2$ couples either to the molecular axis (Hund's case (a)) or to the rotational axis (Hund's case (b)). Transitions between ground and vibrational exited states have to obey the general selection rule, $\Delta\Lambda = 0, \pm 1$, which is valid for both, case (a) and case (b) molecules. Furthermore in addition for Hund's case (a), the projection Ω of spin and electronic angular momentum along the intermolecular axis has to follow $\Delta\Omega = \pm 0, 1$. These rules lead to seven vibronic transitions, four $^2\Sigma$–$^2\Pi$ and three $^2\Delta$–$^2\Pi$. Each transition has a rotational structure with P-, R-, and strong Q-branches. For the Σ state the coupling of the spin to the molecular axis is much weaker and Ω is no longer a good quantum number. With increasing rotational quantum number the electron spin couples to the rotation axis and thus the energy levels are better described as a Hund's case (b). Transitions from case (a) to (b) have a more complicated band structure with less prominent Q-branches. Hougen[25] found that $^2\Sigma$ states behave as Hunds case (a) states when the spin orbit splitting constant A is much larger than both BJ and $\varepsilon\omega$ where ω is the bending frequency, and will behave as case (b) states when A is very much smaller than either BJ or $\varepsilon\omega$. For intermediate situations, the $^2\Sigma$ states will behave in a more complicated fashion. In the case of the ν_5 bending mode ε is

small, a best fit of our simulated spectra to the low resolution spectrum is obtain for $\varepsilon_5 = 0.032$. One finds that $\varepsilon_5\omega_5 = 21$ cm^{-1} is in the order of A and thus the $^2\Sigma$ states belong to an intermediate case between Hund's case (a) and (b). For analysis each of the bands of the $^2\Sigma$–$^2\Pi$ transition can be divided into two sub-bands, $^2\Sigma$–$^2\Pi_{1/2}$ and $^2\Sigma$–$^2\Pi_{3/2}$. A general expression for $^2\Sigma$ energy levels of vibrational state v can be written as (see Herzberg,[26] vol. III, p. 79):

For the upper state, $^2\Sigma^+$:

$$T^+_{[v]}(J) = G + B_{[v]}(J+1/2)^2 + \frac{1}{2}\sqrt{(\Delta\nu)^2 \pm 4B_{[v]}(J+1/2)(v+1)\varepsilon\omega + 4B^2_{[v]}(J+1/2)^2} \quad (6)$$

and for the lower state, $^2\Sigma^-$:

$$T^-_{[v]}(J) = G + B_{[v]}(J+1/2)^2 - \frac{1}{2}\sqrt{(\Delta\nu)^2 \pm 4B_{[v]}(J+1/2)(v+1)\varepsilon\omega + 4B^2_{[v]}(J+1/2)^2}, \quad (7)$$

where G is the ordinary vibrational energy. Although these formulae have been developed for three atomic linear molecules in a $^2\Pi$ electronic state they still hold for linear tetra-atomic molecules, as long as only one of the two bending modes is vibrational excited. $\Delta\nu$ is the expression for the overall splitting between the two Σ states which is defined as:

$$\Delta\nu = \sqrt{A^2 + (v+1)^2\varepsilon^2\omega^2}. \quad (8)$$

In Fig. 3 (upper panel) a Fortrat diagram of the Q-branches is shown. The three Δ–Π transitions are indicated as triangles, whereas crosses are used for the Σ–Π Q-branches. The splitting of the two sub-bands, $^2\Sigma$–$^2\Pi_{1/2}$ and $^2\Sigma$–$^2\Pi_{3/2}$, increases rapidly with the rotational quantum number. Due to the very small Renner–Teller shifts in the Δ state some of the vibronic band centers coincide and it turns out that the main peak at 710 cm^{-1} consists of two Δ–Π transitions which have a considerable overlap in their Q-branches. This pile up effect for the two Q-branches makes the determination of the vibrational frequency rather good and argues that the spin orbit constant for the Π and Δ state are rather similar. Due to this spin orbit coupling of about -30 cm^{-1} the third Δ–Π band appears at about 740 cm^{-1} with a similar rotational structure which is in good agreement with a peak observed at 743 cm^{-1}.

Due to the larger shifts in the Σ states associated with the Renner–Teller effect the Σ–Π transitions have contributions over the range of 667 to 754 cm^{-1}. In addition, simulations show that the four transitions are rather variable in position when varying ε_5. In summary the ro-vibronic structure of the low resolution spectrum is well described by the few spectroscopic constants given in Table 2. Future high resolution spectra will give a more detailed and complete picture of a tetra-atomic Renner–Teller molecule.

4. Kinetic model for LIR of $C_2H_2^+$

The energy level diagram adapted for the LIR-processes of the *cis*-bending vibration ν_5 is shown in Fig. 4. It based upon the results from the spectroscopy section. A similar diagram for the asymmetric stretching vibration ν_3 can be found in reference.[4] The laser induced kinetics starts with the excitation of the ion, *i.e.* reaction (2) at a rate R_{abs}. It has been shown in more detail in the previous LIR study that to first approximation the number of product molecules, *i.e.*, the LIR signal, as a function of the excitation frequency is

$$[C_2H_3^+](\omega)d\omega \sim R_{abs}(\omega)d\omega \sim \rho\mu_{v'v''}{}^2 S_{AB}(\omega)d\omega. \quad (9)$$

Table 2 Spectroscopic constants

Symbol	Value	Remarks
ω_5	(710 ± 4) cm^{-1}	This work[a]
ε_5	0.032	This work[b]
A	−30.91 cm^{-1}	18[c]
B	1.1046 cm^{-1}	18[c]

[a] The error relates to the systematic error in the determination of the absolute value. [b] The error of this quantity is of the order of its value. This is because deficiencies in the simulated spectrum can also be attributed to a variation of spin orbit splitting, A, and the rotational constant, B. In general, good simulated spectra are obtained for $\varepsilon_5 < 0.037$. [c] The spin orbit constant, A, and the rotational constant, B, have been kept constant and equal for all three vibronic states. Their values have been taken from the vibrational ground state as determined by high resolution IR spectroscopy.

Here $\mu_{v'v''}$ is the vibrational dipole moment, a property of the molecular transition under consideration. ρ is the spectral energy density, a property of the exciting laser. $S_{AB}(\omega)d\omega$ is the intensity of the ro-vibronic spectrum. Numbers of important quantities for the simulation of the LIR process are given in Table 1. $\mu_{v'v''}$ for the different vibrational transitions have been derived from the Einstein A coefficient which will be determined independently below from the density dependence of the signal. For ρ in the simulations the cw equivalent value derived from the FELIX parameters during the specific study have been used.

The quantity $S_{AB}(\omega)d\omega$ is related to the Hönl–London factors, $S_{\Omega J'J''}$, of the corresponding transition by the following relation

$$S_{AB}(\omega)\,d\omega = \sum_{\Omega,J'J''} S_{\Omega,J'J''} f(\omega - \omega_{J',J'',\Omega})d\omega. \quad (10)$$

with $f(\omega - \omega_{J',J'',\Omega})d\omega$ the line profile of the individual rotational lines (J',J'') of the vibronic components (Ω), *e.g.* Δ–Π. Due to the normalization of each term the integral is also normalized, $\int S_{AB}(\omega)d\omega = 1$. Because of this normalization, the integrated band intensity of the LIRspectrum, $\int[C_2H_3^+](\omega)d\omega$, is a measure for the product of the square of the vibrational dipole moment, $\mu^2_{v'v''}$ and the rate coefficient for hydrogen abstraction of excited $C_2H_2^+$, k*. In the simulations it has been assumed that k* is a constant for all excited rotational and vibronic states of one vibrational mode. This assumption is of course questionable as there is no *a priori* knowledge on this. However, since the main interest here is the vibrational mode dependence of k*, this is a reasonable first approximation which in future simulations might be easily lifted. As a result, taking the different vibrational dipole moments into account, the ratio of the k* for the two modes has been determined, see Table 1.

When $C_2H_2^+$ is excited, *via* the process described above, it will fluoresce back to the vibrational ground state, with a rate determined by the Einstein A coefficient

$$C_2H_2^+(v_i = 1, J') \xrightarrow{A} C_2H_2^+ + \hbar\omega. \quad (11)$$

While in the excited state, it can collide with a H_2 molecule occurring with the collision rate, k_c, which has been assumed to be its maximum value, the Langevin rate coefficient $k_L = 1.59 \times 10^{-9}$ cm^3 s^{-1}. As a result of the collisions, $C_2H_2^+$ can react to the desired LIR-products with the rate coefficient k*, reaction (3), or it can be quenched

$$C_2H_2^+(v_i = 1, J') + H_2 \xrightarrow{k_{rlx}} C_2H_2^+(v_i = 0, J'') + H_2. \quad (12)$$

In the simple model described here, it is assumed that every collision leads to either reaction or quenching, *i.e.* $k_L = k^* + k_{rlx}$. In ref. 4, it has been found that for the acetylene

cations excited in the stretching motion the reaction and quenching rate coefficients are $k^* \sim (1/6)k_L$ and $k_{rlx} \sim (5/6)k_L$.

As mentioned in eqns. (4) and (5), one has also to account for the loss of primary ions by radiative and ternary association processes leading to the formation of $C_2H_4^+$. The corresponding reactions are denoted as $k_{ass} = k_{rad} + k_{ter}$ [H_2] in Fig. 4. The values used for the association rate coefficients at a temperature of 90 K have been measured independently to be on the order of $k_{rad} = 10^{-13}$ cm^3 s^{-1} and $k_{ter} = 10^{-25}$ cm^6 s^{-1}.[27]

These above described processes, characterized by their rate coefficients or rates, have been numerically simulated by following the number of the species $C_2H_2^+(v = 0)$, $C_2H_2^+(v = 1)$, $C_2H_3^+$ and $C_2H_4^+$ in time. For the initial conditions at time zero, the time when the ions enter the trap, the number of primary $C_2H_2^+(v = 0)$ ions and background $C_2H_3^+$ ions have been set to the measured values. Usually there were 2000 $C_2H_2^+$ ions and about 200 $C_2H_3^+$ generated by hot $C_2H_2^+$ ions entering the trap. The time development has then been obtained by setting up a coupled rate equation system containing the five processes in Fig. 4, and doing small time steps (on the order of μs), in which the infinitesimal number changes due to the processes have been subtracted or added to the number of the involved species. As mentioned above, in this numerical procedure the laser has been treated to operate in cw mode for simplicity. If necessary, the simulations could be extended to include processes like stimulated emission of one photon from the upper vibrational level or rotational inelastic collisions. These numerical simulations are presented in the following sections together with the experimental results.

5. Measurements and kinetics results

Several systematic studies of the LIR-signal dependencies have been carried out. In first approximation, the LIR-signal should increase with the number of primary ions, the number density of H_2 target molecules, the trapping time and the laser intensity. But as the preceeding section showed, the occurring processes can be quite complex, thus the measurements were accompanied by numerical simulations applying the presented simple kinetic model. These measurements and simulations served not only to guarantee that the measured $C_2H_3^+$ signal originated from the successive processes described in eqns. (2) and (3), but also to extract valuable parameters such as radiative lifetimes and reactivities.

At first it was verified for the bending vibration that the laser induced increase of daughter ions $C_2H_3^+$ is correlated with a decrease of parent ions $C_2H_2^+$. Furthermore, the dependence

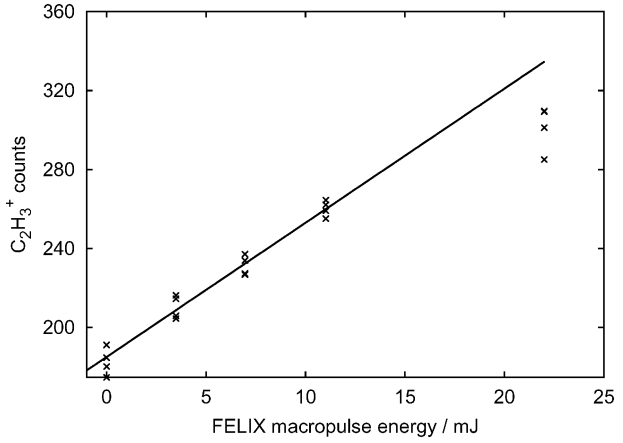

Fig. 5 Dependence of the LIR-signal for the *cis*-bending vibration at 710 cm^{-1} on laser power. The primary $C_2H_2^+$ ions have been stored at 90 K in 1.6×10^{11} cm^{-3} H_2 and exposed to the 10 Hz laser pulses. After 3 s storage time, the $C_2H_3^+$ product ions have been counted and the laser power has been varied by means of an attenuator. The $C_2H_3^+$ counts for zero laser power are due to hot $C_2H_2^+$ parent ions coming from the ion source.

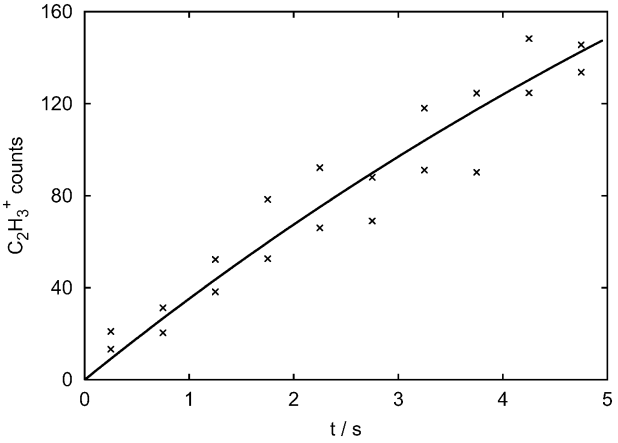

Fig. 6 Dependence of the LIR-signal for the bending vibration on the storage time *t*. In this experiment, the primary ions have been stored at 90 K in 1.5×10^{11} cm^{-3} H_2 and exposed to the laser pulses (10 Hz, 20 mJ, 710 cm^{-1}) for varying storage times *t*. The solid line represents a numerical simulation as in Fig. 7.

on laser power has been carefully checked. Fig. 5 shows the number of $C_2H_3^+$ products as a function of the pulse energy at a fixed laser frequency (710 cm^{-1}, 10 Hz repetition rate), a trapping time of 3 s and a H_2 number density of 1.6×10^{11} cm^{-3}. Tuning of the laser power has been achieved by the use of calibrated, selectable attenuators integrated into the FELIX beamline. Linearity of these attenuators has been checked independently. The LIR-signal shows a linear power dependence for pulse energies up to 15 mJ pulse^{-1}. This shows that LIR is associated with the absorption of one photon as described in eqn. (2). For higher pulse energies some saturation of the process becomes visible. This saturation of the LIR-signal is probably associated with the fact that at a high instant laser power of FELIX stimulated emission processes are starting to play a role.

It is obvious that the LIR signal should also exhibit a linear increase with trapping time as the number of collisions increases. Fig. 6 shows the number of $C_2H_3^+$ products as a function of the storage time at a fixed laser frequency (710 cm^{-1}), a constant laser power (20 mJ/macropulse, 10 Hz repetition rate) and a H_2 number density of 1.5×10^{11} cm^{-3}. The LIR signal increases linearly with trapping time. A simulation of the reaction kinetics leads to the solid line which exhibits a small nonlinear contribution. It has been checked in the numerical calculations that this slight curvature is only related to the influence of the association processes (eqns. (4) and (5)), by which the parent ions are lost to $C_2H_4^+$ products.

Also the correlation with the number of primary ions has been checked. Special care has been taken that only the number of primary ions was varied while leaving all other experimental conditions invariant. For this purpose the trapping potential of the storage ion source has been varied. Disabling the storage capability of the ion source in this way lead to a total disappearance of the $C_2H_3^+$ counts. This procedure made sure that the same amount of spurious neutral C_2H_2 from the source chamber could reach the trap. Special care had to be taken about the neutral acetylene since the spectra of the bending vibration of the neutral, centered around 730 cm^{-1}, and the ionic species partly overlap. Even assuming a 100% excitation efficiency for the neutral acetylene it becomes clear that at the low densities of neutral acetylene in the trap chamber the "poor" duty cycle of the laser excitation leads to vanishing contributions of a charge transfer from the cold trapped $C_2H_2^+$ ions to the excited neutral acetylene which, by a secondary reaction with H_2, could lead to $C_2H_3^+$ products. In the 22-pole ion trap, excited neutrals are always rapidly relaxed by collisions with the walls.

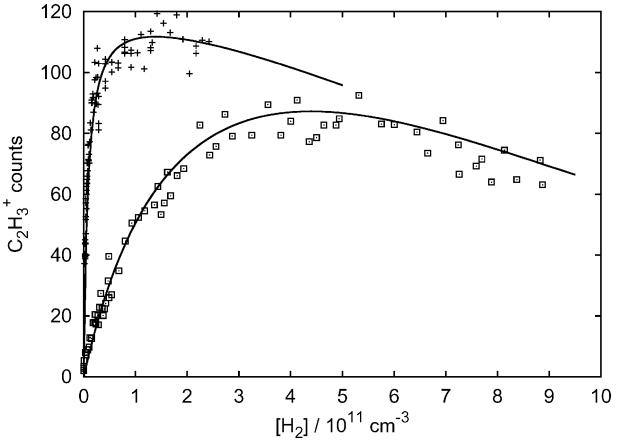

Fig. 7 Density dependence of the $C_2H_3^+$ counts measured at the center frequencies of the two investigated molecular vibrations (crosses: *cis*-bending, squares: asymmetric stretch). In this experiment, about 1800 $C_2H_2^+$ ions have been stored for 3 s and exposed to the laser light. The pulse energy has been about 27 mJ at 10 Hz repetition rate and 710 cm^{-1} as well as 6 mJ at 5 Hz repetition rate and 3135 cm^{-1}. Numerical simulations including five contributing processes (laser excitation, fluorescence, reaction, association, and relaxation) are shown as solid lines. The lifetimes τ resulting from this simulation are summarized in Table 1.

Finally the correlation with the neutral H_2 target gas has been determined. The density dependence of the LIR-signals for the *cis*-bending and the C–H stretching vibrations is displayed in Fig. 7. In both cases the density dependence is characterized by a linear increase, followed by a saturation and a further decrease of the signal at higher H_2 number densities. Numerical calculations have been applied to reproduce this complex behavior using the model described in Section 4 and depicted in Fig. 4. The resultant simulations are shown as solid lines in Fig. 7. In these calculations, the laser absorption rates R_{abs} for ν_3 and ν_5, the association rate coefficients k_{ass}, $k_{rad} + k_{ter}[H_2]$, and the Langevin collision rate coefficient k_L have been used as given in Section 4. The number of initial ions N_0 injected into the 22-pole trap were around 1800 for both vibrational cases.

As it turns out, the shape of the LIR-signal for low densities depends predominantly on the radiative lifetime τ of the excited vibration (as long as $1/\tau$ is much larger than the collision frequency, $k_L[H_2]$). On the other side, parameters like the initial number of parent ions N_0, the absorption rate R_{abs}, the LIR rate coefficient k^*, and the fraction of pumped states g, determine the magnitude of the signal in the saturation region. In fact simulations only serve to determine the value of the product of these quantities. Therefore it is necessary to determine the individual parameters separately. For R_{abs} this becomes possible due to the link to the radiative lifetime τ (see below). Once saturation of the LIR-signal is reached, it decreases for higher H_2 number densities due to increasing loss reactions into ternary association (5), which is nicely reproduced in the simulation. These facts have been used to obtain values for the lifetimes τ of the bending and stretching vibrations of $C_2H_2^+$.

For the stretching vibration, a radiative lifetime of $\tau_3 = (3 \pm 1)$ ms is obtained from the numeric simulation. Similar systematic measurements for this vibrational mode have been conducted in a previous series of experiments[4] where a difference frequency scheme has been employed to generate the appropriate IR radiation. It is gratifying that the corresponding experiments using FELIX lead to the same quantitative result. For the lower-energy bending vibration, a longer lifetime is expected and also measured, as can be seen on the much steeper increase of the signal in Fig. 7. Its lifetime is determined to be on the order of $\tau_5 = (200 \pm 50)$ ms. Apparently the determination of longer lifetimes τ turns out to be less sensitive in the simulations. Nevertheless it is clear that τ_5 is much longer than τ_3. Based on the ω^3-dependence of A, the corresponding dipole moments for the bending and stretching vibration are very similar. The corresponding Einstein A coefficients, $A = 1/\tau$, have been used to determine the vibrational transitions dipole moments, see Table 1, and together with ρ, the absolute value for R_{abs}. As a final result the product of the LIR rate coefficient k^* and the fraction of pumped states can be determined from the simulations. Therefore it is difficult to determine the reactivity of the two vibrational modes. Additional modelling of the population of the rotational states would be necessary. This problem has been solved by comparing the integrated band intensities. In this case all states are pumped at some stage and therefore the ratio compares the two rate coefficients as desired.

Although the trap apparatus has been the same in all LIR-experiments some uncertainties arise from the fact that the laser power is measured prior to entering the trap apparatus. In addition the different time profiles of the laser schemes used here and in the previous study should also be taken into account. It has been seen from Fig. 5 that saturation effects start to play a role. Further investigations along this line are necessary. Despite this open question it is interesting to compare the reactivity of the two modes. The rate coefficient k_5^* has been determined to be a factor of about ten smaller than k_3^*. Some dynamical restrictions may be associated with this finding and will be discussed in the following.

6. Discussion and conclusion

Two major results arise from the present LIR study. (i) From the spectrum of the *cis* bending vibration it can be concluded that the Renner–Teller parameter is rather small. (ii) The rate coefficient for hydrogen abstraction is strongly mode dependent, highly in favor of the C–H stretching mode when compared to the bending vibration. Due to the limited resolution of FELIX the absolute value of ε_5 has to be taken with some care, especially since several assumptions on the other spectroscopic constants have been made. In order to lift these uncertainties it will be necessary to detect a LIR-spectrum using a high resolution laser. First attempts using a diode laser system were unsuccessful, probably since the spectral energy density of the diode laser is smaller than that of FELIX and also because only a single state of the parent molecule is excited at a time. Thus the partition function can be rather unfortunate in case of the finite number of parent molecules in the trap. One obvious way to remedy this problem is to conduct the experiment at low temperatures, *e.g.* 10 K, which are accessible in the trap apparatus. A LIR signal for low temperatures has been detected when the stretching vibration was excited. However, as an additional surprising result no sufficient LIR signal could be detected for the bending vibration at temperatures below 50 K.

At the low collision energies of the trap experiment it is common to assume that any reaction of $C_2H_2^+$ with hydrogen proceeds *via* an intermediate complex. Complex lifetimes for ground state $C_2H_2^+ \cdot\cdot H_2$ have been determined from rate coefficients for ternary association. At 90 K the lifetime is of the order of a microsecond.[28] These complexes represent intermediate states to the $C_2H_4^+$ molecule which is bound by 2.6 eV.[29] The reverse reaction of $C_2H_4^+$ to $C_2H_2^+ + H_2$ occurs as well at the appropriate excitation energies.[30] H-atom scrambling is a process which occurs readily in the $C_2H_2^+ \cdot\cdot H_2$ complex and also in the decomposition of the $C_2H_4^+$. This scrambling mediates an effective isotope exchange of $C_2H_2^+$ in collisions with HD which under interstellar conditions leads to the well known isotopic fractionation of $C_2H_2^+$.

In the present as well as in the previous study[4] also the LIR process of the vibrationally excited $C_2H_2^+$ has been assumed to

proceed *via* a collision complex. According to the Langevin–Gioumousis–Stevenson capture theory[31] such a complex is formed irrespective of the vibrational excitation of the parent ion. Its lifetime with respect to decomposition, τ_{dis} may, however, strongly depend on the excitation state. The present analysis is based on this simple mechanism. Most sensitively the simulations of the density dependencies shown in Fig. 7 react on changes of the rate coefficients. In fact the fluorescence lifetimes would vary substantially giving in on the assumption of a complex formation at a rate coefficient of k_L. On the contrary the good agreement of the fluorescence lifetime of the C–H stretch vibration with theoretical predictions by Lee *et al.*[13] foster the assumptions made.

As pointed out already in the introduction, rather similar results concerning the mode dependence of the reaction of $C_2H_2^+$ with hydrogen have been obtained in a series of detailed guided ion beam experiments by Chiu *et al.*[19] Effects of vibrational excitation and collision energy on the cross sections and branching ratios for the reaction of $C_2H_2^+$ with D_2 have been studied and reveal that C–C stretching vibration enhances the reaction rate while bending vibration does not. The interpretation of the branching ratios for the different isotopic reaction channels is based on the formation of an intermediate complex. The inhibition of the reaction in case of the bending vibration has been associated with a bottleneck in the entrance channel which circumvents the complex formation. This interpretation, that the complex might not be formed is quite different from the scenario drawn here: The complex forms, however, quenching of the vibrationally excited state is rather efficient. On the contrary reaction would in effect only play a minor role.

One possible reason for finding this branching fraction is that quenching reduces the lifetime of the excited species which has sufficient energy to overcome the endothermicity of reaction. In case of the C–H stretching vibration quenching to the vibrational ground state is already many times more efficient than reaction. The same number of products would be detected if one would assume that the complex would only be formed in a small fraction of the cases but reaction would proceed with 100% efficiency. However, a simple analytical expression for the number of product molecules as a function of the H_2 number density can be derived. In first approximation this number rises as k^* $[H_2]/(A + (k^* + k_{rlx})[H_2])$, with A the Einstein A-coefficient and $(k^* + k_{rlx})[H_2]$ the total rate at which the excited state is depopulated. In the present case $(k^* + k_{rlx}) = k_L$ has been assumed. In contrast, the assumption of a hindered complex formation is represented by $(k^* + k_{rlx}) \ll k_L$. It is obvious that both assumptions lead to largely different fluorescence lifetimes, $\tau = 1/A$. Therefore they are quite distinct.

Under the assumption $k^* \ll k_{rlx} \sim k_L$, which is in agreement with the complex formation scenario, the branching ratio could also be explained by a mode dependence of k^*. When discussing this mode dependence it has to be taken into account that hydrogen abstraction is an endothermic process and that the excitation of the ν_3 mode supplies about four times more energy than excitation of the ν_5 mode. An effective temperature increase as a result of the laser excitation can be calculated on the basis of the heat capacity of the $C_2H_2^+ \cdot \cdot H_2$ complex and under the assumption that the vibrational energy added to the parent ion is redistributed in the collision complex during its lifetime. Taking into account the endothermicity of reaction a ratio of about four for k_3^*/k_5^* is determined using an Arrhenius type expression to model k^*. This ratio compares reasonably well with the ratio determined from experiment. Therefore the mode dependence of k^* could be explained on the basis of energetic reasoning. On the contrary, no specific mechanistic mode dependence is necessary. This interpretation is in agreement with the concept of complex formation. In fact the lifetime of the collision complex is long compared to timescales related to internal motions. Therefore no memory effects on the excitation mode is expected under these conditions and details of the potential energy surface would not play a significant role for the outcome of the reaction. As a consequence no specific dynamical restrictions leading to a mode dependence are expected. The present results are consistent with this scenario. However, care has to be taken when drawing final conclusions.

Five processes have been accounted for in the kinetics model simulating the LIR-process. When trying to unravel the nature of the mechanisms at work during collision it might be necessary to include even more processes or the ones used to a greater detail. One example is the explicit treatment of the time structure of the exciting laser, another the rotational redistribution of the hole in the ground state population which appears upon laser excitation. A third process which might be of some importance concerns rotationally inelastic collisions within the vibrational excited species. LIR-experiments with more specific excitation, in particular high-resolution studies are necessary to obtain a more detailed understanding. Based on the fact that the value for the fluorescence lifetime for the stretching vibration is in rather good agreement with theory one would hope that high quality *ab initio* calculations of IR intensities also for the bending vibration will be conducted. Such a value could be used in a refined simulation of the current experiments. As a result it could be possible to conclude that complex formation might indeed be inhibited for the bending vibration, whereas the competition between quenching and reaction governs the role of the stretching vibration.

It becomes clear from this study that LIR is a very useful tool for spectroscopy of ions as well as for the dynamics of ion–molecule reactions. Other interesting examples for LIR-experiments involve complex molecules such as CH_5^+, C_3H^+ and other carbon containing species. Also more general reaction schemes as discussed in ref. 2 can enlarge the number of ions accessible to LIR.

Acknowledgements

Financial support by the Deutsche Forschungsgemeinschaft (DFG) is gratefully acknowledged, especially *via* the Forschergruppe FOR 388 ''Laboratory Astrophysics'' and *via* project GI 319/1-2 within the framework of the European Associated Laboratory for High Resolution Spectroscopy (LEA HiRes). We gratefully acknowledge the support by the Stichting voor Fundamenteel Onderzoek der Materie (FOM) in providing the required beam time on FELIX and highly appreciate the skilful assistance by the FELIX staff (René van Buuren, Lex van der Meer, Britta Redlich). Furthermore the authors thank for the excellent support by the electronic and mechanical workshops of Leiden university (Ewie de Kuyper, Koos Benning, René Overgrauw). O.A. thanks Ewine van Dishoeck for financial support.

References

1 O. Asvany, S. Schlemmer, B. Redlich, P. Kumar, I. Hegelmann and D. Marx, submitted to *Nature*.
2 S. Schlemmer and O. Asvany, *J. Phys.: Conf. Ser.*, 2005, **4**, 134–141.
3 S. Schlemmer, T. Kuhn, E. Lescop and D. Gerlich, *Int. J. Mass Spectrom.*, 1999, **185**, 589–602.
4 S. Schlemmer, E. Lescop, J. v. Richthofen and D. Gerlich, *J. Chem. Phys.*, 2002, **117**, 2068–2075.
5 O. Asvany, T. Giesen, B. Redlich and S. Schlemmer, *Phys. Rev. Lett.*, 2005, **94**, 73001-1–73001-4.
6 S. T. Pratt, P. M. Dehmer and J. L. Dehmer, *J. Chem. Phys.*, 1993, **99**, 6233–6244.
7 J. Reutt, L. Wang, J. Pollard, D. Trevor, Y. Lee and D. Shirley, *J. Chem. Phys.*, 1986, **84**, 3022–3031.
8 P. Dehmer and J. Dehmer, *J. Electron. Spectrosc. Relat. Phenom.*, 1982, **28**, 145.

9 T. M. Orlando, S. L. Anderson, J. R. Appling and M. G. White, *J. Chem. Phys.*, 1987, **87**, 852–860.
10 S. T. Pratt, P. M. Dehmer and J. L. Dehmer, *J. Chem. Phys.*, 1991, **95**, 6238–6248.
11 Y. F. Zhu, R. Shehadeh and E. R. Grant, *J. Chem. Phys.*, 1999, **99**, 5723.
12 A. N. Petelin and A. A. Kiselev, *Int. J. Quantum Chem.*, 1972, **6**, 701.
13 T. J. Lee, J. E. Rice and H. F. Schaefer, III, *J. Chem. Phys.*, 1987, **86**, 3051–3053.
14 M. Perić, S. Peyerimhoff and R. Buenker, *Mol. Phys.*, 1985, **55**, 1129.
15 M. Perić and S. D. Peyerimhoff, *J. Chem. Phys.*, 1995, **102**, 3685–3694.
16 M. Perić, H. Thümmel, C. M. Marian and S. D. Peyerimhoff, *J. Chem. Phys.*, 1995, **102**, 7142–7149.
17 M. W. Crofton, M. F. Jagod, B. D. Rehfuss and T. Oka, *J. Chem. Phys.*, 1987, **86**, 3755.
18 M.-F. Jagod, M. Rösslein, C. M. Gabrys, B. D. Rehfuss, F. Scappini, M. W. Crofton and T. Oka, *J. Chem. Phys.*, 1992, **97**, 7111–7123.
19 Y.-H. Chiu, B. Yang, H. Fu, S. L. Anderson, M. Schweizer and D. Gerlich, *J. Chem. Phys.*, 1992, **96**, 5781–5788.
20 K. Honma, T. Kato, K. Tanaka and I. Koyano, *J. Chem. Phys.*, 1984, **81**, 5666.
21 D. Gerlich, in *State-Selected and State-to-State Ion-Molecule Reaction Dynamics*, ed. C.-Y. Ng and M. Baer, 1992, vol. LXXXII, pp. 1–176.
22 D. Oepts, A. van der Meer and P. van Amersfoort, *Infrared Phys. Technol.*, 1995, **36**, 297–308.
23 M. Jacox, *J. Phys. Chem. Ref. Data.*, 1994, **3**.
24 M. Perić and S. D. Peyerimhoff, *J. Mol. Spectrosc.*, 2002, **212**, 142–152.
25 J. T. Hougen, *J. Chem. Phys.*, 1962, **36**, 519–534.
26 G. Herzberg, *Molecular Spectra and Molecular Structure III*, Krieger Publishing Company, Malabar, FL, 1991.
27 D. Gerlich, *J. Chem. Soc., Faraday Trans.*, 1993, **89**, 2199–2208.
28 A. Sorgenfrei, *Ion-Molekül-Reaktionen kleiner Kohlenwasserstoffe in einem gekühlten Ionen-Speicher*, PhD thesis, University of Freiburg, Germany, 1994.
29 R. Stockbauer and M. G. Inghram, *J. Chem. Phys.*, 1975, **62**, 4862–4870.
30 M. Malow, F. Güthe and K.-M. Weitzel, *Phys. Chem. Chem. Phys.*, 1999, **1**, 1425.
31 G. Gioumousis and D. Stevenson, *J. Chem. Phys.*, 1958, **29**, 294.

